

Kinetic Studies of Isoprene Reactions Initiated by Chlorine Atom

Inseon Suh and Renyi Zhang*

Department of Atmospheric Sciences, Texas A&M University, College Station, Texas 77843

Received: February 15, 2000; In Final Form: May 15, 2000

The degradation reactions of isoprene initiated by chlorine atom were investigated using a fast-flow reactor coupled to chemical ionization mass spectrometry (CIMS) detection. The kinetic studies were performed in the pressure range of 5 to 10 Torr and at 298 ± 2 K. The rate constant for the reaction between Cl and isoprene was measured to be $(4.0 \pm 0.3) \times 10^{-10} \text{ cm}^3 \text{ molecule}^{-1} \text{ s}^{-1}$. Using the CIMS method, we were able to directly detect the products of the Cl–isoprene reaction, HCl and Cl–isoprene adduct. A branching ratio of $(17.4 \pm 4.0)\%$ was determined for the HCl formation. We have also measured the rate constant for the reaction of the Cl–isoprene adduct with molecular oxygen to form the β -chloroalkenylperoxy radicals, with a value of $(1.0 \pm 0.3) \times 10^{-14} \text{ cm}^3 \text{ molecule}^{-1} \text{ s}^{-1}$. Atmospheric implications of the present experimental results are discussed.

Introduction

Due to its high chemical reactivity and proliferation in the generation of organic peroxy radicals, isoprene (2-methyl-1,3-butadiene, $\text{CH}_2=\text{C}(\text{CH}_3)\text{CH}=\text{CH}_2$) plays an important role in ozone formation in local and regional atmosphere.^{1–7} Atmospheric oxidation of isoprene can be initiated by reactions with a variety of oxidant species, among which the hydroxyl radical OH is the most important. Reactions of isoprene with ozone, nitrate radical NO_3 , and halogen atoms and their oxides can also be important and may in some cases give a larger contribution to the oxidation rate than OH.⁸ For example, it has been suggested that reactive chlorine may play a potential role in the photochemical oxidation of hydrocarbons.⁹ Reactive chlorine is produced in the atmosphere both as a consequence of direct emission and of multiphase chemical processes.¹⁰ Four major sources of reactive chlorine have been identified: oceanic and terrestrial biogenic emissions, sea-salt production, and dechlorination, biomass burning, and anthropogenic emissions. Indications for a significant role of chlorine atoms in the marine boundary layer have been obtained through field measurements of the relative degradation rates of saturated hydrocarbons, which show a significant deviation from what can be explained by OH radical chemistry.^{11–13} Also, high concentrations of chlorine atoms have been implicated in the depletion of surface ozone during the arctic spring.^{11,12} Other potentially important chlorine chemistry in the oxidation of hydrocarbons has also been suggested. Assuming a peak Cl concentration of $1.4 \times 10^5 \text{ atoms cm}^{-3}$, the lifetime of some of the smaller alkanes would be about 14 h, in contrast to 253 h for the oxidation by OH at the OH concentration level of $10^6 \text{ molecules cm}^{-3}$.^{12–14} On the other hand, the chlorine radicals may play a minor role in the oxidation of alkanes on the global scale, due to the relatively small concentrations of chlorine atoms.^{15–17}

Recently, several laboratory studies have investigated the kinetics and mechanism of the oxidation reactions of isoprene initiated by Cl atoms. The rate constants between isoprene and Cl have been studied using both a relative rate method^{18–20} and absolute rate measurements.^{21,22} The pressure dependence of

the Cl–isoprene reaction has been investigated in the pressure range of 0.1 to 760 Torr.^{18,21,22} Some of those studies have also identified the reaction products,^{18–20,22} including CO, CO_2 , formyl chloride, formic acid, methyl-glyoxal, and hydrogen chloride. Other likely end products of the isoprene reactions include α,β -unsaturated carbonyls (methyl vinyl ketone and methacrolein).^{18,19} In addition, the rate constant for the reaction between Cl and isoprene and the HCl formation yield has been investigated as a function of temperature in the range 230–320 K.²² At present, however, there are some controversies regarding the initial reaction of isoprene with chlorine atom. For example, the work by Notario et al.²¹ and Bedjanian et al.²² concluded that this reaction is pressure independent at pressures as low as 0.3 Torr, in contrast to the findings by Ragains and Finlayson-Pitts.¹⁸ Also, there is a disagreement in the reported rate constants among the various studies, with values ranging from $(3.6 \text{ to } 5.6) \times 10^{-10} \text{ cm}^3 \text{ molecule}^{-1} \text{ s}^{-1}$.

The mechanism of the atmospheric photochemical oxidation of isoprene initiated by chlorine atom has been tentatively proposed.^{18,19} The initial reaction between isoprene and Cl proceeds mainly by Cl addition (1b), forming the Cl–isoprene adduct radical.



Under atmospheric conditions, the Cl–isoprene adduct is expected to react primarily with oxygen molecules to form the β -chloroalkenylperoxy radicals. In the presence of nitric oxide NO, initial Cl radical addition at the 1-, 2-, 3-, or 4-positions with subsequent addition of O_2 at the 2-, 1-, 4-, and 3-positions, respectively, leads to the formation of β -chloroalkenylalkoxy radicals. The dominant tropospheric reaction of the β -chloroalkenylalkoxy radicals is believed to be decomposition or reaction with oxygen molecule, leading to the formation of various oxygenated and nitrated organic compounds. Alternatively, isoprene also undergoes methyl–hydrogen abstraction to form HCl and an allylic radical (1a). The branching ratio for the initial reaction has been inferred from the HCl formation yield, with values between 13 and 17%.^{18,22} A mechanistic

* To whom correspondence should be addressed.

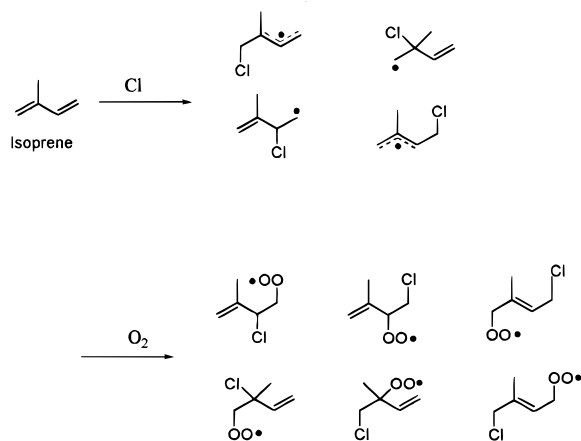


Figure 1. Mechanistic diagram for the reactions of Cl with isoprene and the Cl–isoprene adduct with O₂.

diagram for the reaction of Cl with isoprene to form the Cl–isoprene adduct radicals and the subsequent reaction of the adducts with O₂ to form the β-chloroalkenylperoxy radicals is shown in Figure 1.

Currently direct experimental data concerning the intermediate processes of the oxidation reactions of isoprene are very limited. There are few experimental studies available on the chemistry of the radical intermediates. Absolute or relative rate constants for the subsequent reactions of these intermediate radicals are not available. Our understanding of the atmospheric oxidation mechanism of isoprene is primarily based on the environmental chamber investigations to identify the final products of the reactions.^{18,19} Clearly, an accurate and complete knowledge of the atmospheric chemistry of isoprene is required to understand air pollution in urban and regional environments.

In this study, we report laboratory kinetic studies of the reactions of isoprene initiated by chlorine atom Cl. The rate constant of the reaction of Cl with isoprene has been measured in the pressure range of 5 to 10 Torr and at the temperature of 298 ± 2 K. Using the CIMS method, we were able to directly detect the reaction products, hydrogen chloride, and the Cl–isoprene adduct. The reaction products were used to obtain the branching ratio of the initial reaction of Cl with isoprene. We have also investigated the reaction of the Cl–isoprene adduct with molecular oxygen to form the β-chloroalkenylperoxy radicals.

Experimental Section

A fast-flow reactor, in conjunction with chemical ionization mass spectrometry (CIMS) detection, was used in the present experiments. A schematic of the experimental setup is shown in Figure 2. The flow reactor was constructed from precision-bore Pyrex tubing 1.78 cm internal diameter and 120 cm in length. All surfaces exposed to the reactants and products were coated with a halocarbon wax. A flow of a He carrier gas (in the range of 1 to 3 STP l min⁻¹) was injected to the flow reactor through an entrance port in the rear of the flow reactor. The pressure of the flow reactor was regulated between 5 and 10 Torr, and the temperature of the flow reactor was at 298 ± 2 K. Typical flow velocity in the flow reactor ranged from 1300 to 2500 cm s⁻¹. A high capacity mechanical pump (1400 l min⁻¹) was used to evacuate the flow reactor. Pressures in the flow reactor were monitored by two capacitance manometers (10 and 1000 Torr full scales). Isoprene was added to the flow reactor through a series of five addition ports located 5 cm apart at the downstream end of the flow tube. The reactant addition

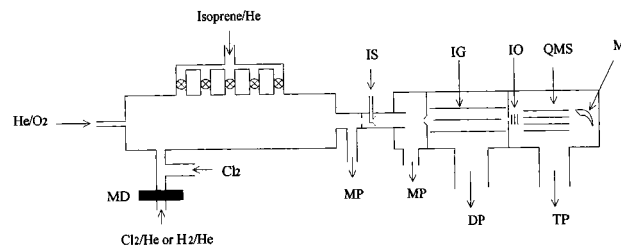


Figure 2. Schematic diagram of the fast-flow reactor/CIMS system: DP = diffusion pump, IG = ion guide, IO = ion optics, IS = ion source, M = multiplier, MD = microwave discharge, MP = mechanical pump, QMS = quadrupole mass spectrometer, and TP = turbo molecular pump.

ports were designed to minimize disturbance of the viscous flow. At each of the ports, a hole of about 2 millimeters in diameter was drilled on the wall of the reactor tube. The hole was enclosed in a Pyrex sleeve which was sealed to the reactor tube. Glass vacuum valves with Teflon plugs were used to control the flow of reactants at each of the addition ports.

The flow reactor was operated under the laminar flow condition with Reynolds number $Re = 2aup/\mu$ in the range of 10 to 30, where a is the internal radius of the flow reactor, ρ the density of the gas, u the flow velocity, and μ the viscosity coefficient of the gas. Under our experimental conditions, the entrance length for the flow to fully develop a parabolic velocity profile can be estimated with the relation $l = 0.115aRe$.²³ Using a typical value of 25 for the Reynolds number relevant to our experimental conditions, this length was determined to be about 3 cm, significantly shorter than that of the flow reactor. A laminar flow was hence fully developed under our laboratory conditions. The mixing times for Cl and isoprene can be estimated using $t_{mix} = a^2/(5D)$.²³ At 298 K the values of the pressure-independent gas-phase diffusion coefficients, PD , are 602 and 365 Torr cm² s⁻¹ for Cl and isoprene in helium, respectively.²³ Using the typical flow velocity in our experiments, those led to the mixing lengths of 6 and 8 cm for these two species. Hence, homogeneous mixing of both Cl and isoprene was effectively achieved in our experiments.

Reactants and products of the isoprene reactions were detected by CIMS using either positive or negative reagent ions. The CIMS employed a new approach, involving an electrostatic ion guide recently developed.^{24,25} Gases from the flow reactor were introduced into the ion–molecule reaction region. Positive or negative reagent ions were initiated using corona discharge at a high voltage (5 kV). The SF₆⁻ reagent ions were generated by adding a small amount of SF₆ to a He carrier flow (about 1–2 slpm at STP) through the discharge. The positive reagent ions O₂⁺ were produced by passing the He carrier flow through the discharge and then adding a small amount of O₂ downstream. A small portion of the ion/gas flow from the ion source was drawn into the next vacuum stage through a 0.5 mm orifice. An electrostatic ion guide was used to transport ions to another orifice leading to the quadrupole mass analyzer. The chambers housing the ion guide and the mass spectrometer were evacuated by a diffusion pump and a turbomolecular pump, respectively. The use of the ion guide allows for both ion transportation with a high efficiency and preferential separation and removal of neutral molecules in a differential pumping system.^{24,25} Detection sensitivity of our CIMS system was generally in the range of 10⁷ to 10⁸ molecules cm⁻³ with a S/N ratio of unity for a one second integration time, independent of pressure. The high detection sensitivity of our CIMS approach enabled monitoring of trace species formed during the isoprene oxidation reactions.

Two different approaches were employed to generate, in situ, the chlorine atom. First, Cl radicals were generated by passing a small flow of (0.1–1)% Cl₂/He mixture through a microwave discharge. Alternatively, we passed a small flow of (0.1–1)% H₂/He mixture through the microwave discharge and then added an excess of molecular chlorine downstream



The kinetic results obtained using these two methods were similar within the uncertainty of our experiments. The former method was used in the majority of the experiments reported in this study. Cl was detected in the negative ion mode using SF₆[−] as the reagent ions, according to the ion–molecule reaction



The ion–molecule reaction rate for reaction 3 has not been measured. The Cl concentration was determined using the titration reaction



$$(k = 2.3 \times 10^{-10} \exp\{-(135 \pm 60)/T\} \text{ cm}^3 \text{ molecule}^{-1} \text{ s}^{-1})$$

with an excess of Br₂.²² In this case, the Cl concentration was derived according to [Cl] = Δ[Br₂] = [ClBr]. Alternatively, we also inferred the chlorine atom concentrations by determining the concentrations of chlorine molecules introduced to the flow reactor, according to [Cl] ≈ 2Δ[Cl₂], where Δ[Cl₂] is the difference in the chlorine concentrations when the microwave discharge was switched off and on. The flow-through quartz cell used in the Evenson cavity was coated with a concentrated phosphoric acid to enhance the dissociation efficiency of the chlorine molecules. Typically, the concentration of chlorine atoms in the flow reactor was estimated in the range of (1 to 5) × 10⁹ molecule cm^{−3}.

Commercially available isoprene (Aldrich 99.5%) was introduced to the flow reactor by passing He through a bubbler held at the dry ice/acetone temperature. Gaseous isoprene was added to the flow reactor along with a small He flow (0.1 to 10 cm³ min^{−1} at STP) and further diluted in the main helium carrier flow. Isoprene in the flow reactor was calibrated according to the vapor pressure expression of pure isoprene of log *P* = 7.85 − 1511.41/*T* and the dilution factor of the isoprene flow. Alternatively, we volumetrically prepared a 1% isoprene mixture with He in a 2-liter glass bulb and then introduced the isoprene mixture into the flow reactor using a 10 sccm flow meter to verify the isoprene calibration.²⁶ The concentrations of isoprene in the flow reactor were regulated in the range of 10¹⁰ to 10¹¹ molecule cm^{−3}, which were at least a factor of 10 higher than the Cl concentration to ensure the pseudo-first-order kinetic assumption. Isoprene was detected by the CIMS using positive reagent ions, as either the deprotonated [M − H]⁺, the parent [M]⁺, or the protonated [M + H]⁺ isoprene ions. For both Cl and isoprene, the mass spectrometer signals were linear over the range of the concentrations used.

Mass flow meters (Tylan General) were used to monitor all of the flows introduced into the flow reactor. The following gases were used without further purification: He (99.999%), O₂ (99.994%), H₂ (99.999%), and Cl₂ (99.99%).

Results and Discussions

Isoprene Reaction with Cl. The kinetics of the reaction of isoprene with Cl was studied based on the pseudo-first-order

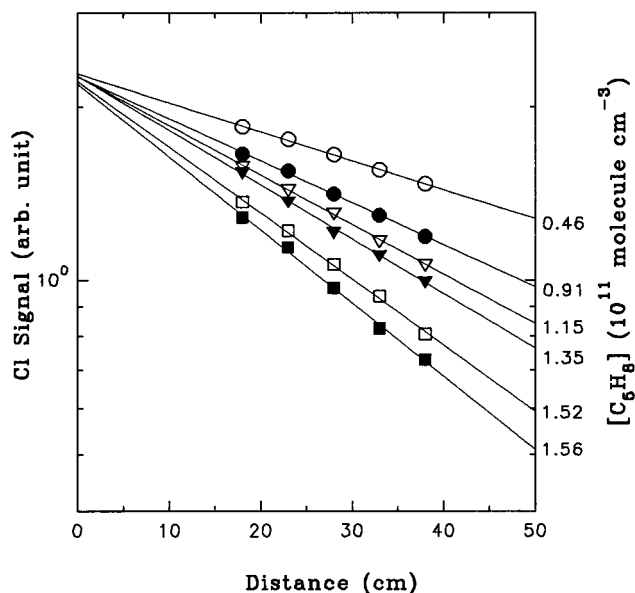


Figure 3. Decay of Cl signal as a function of injector distance at various concentrations of isoprene. Experimental conditions are: *P* = 8.7 Torr, *U* = 2301, and *Re* = 23.

approximation, using isoprene as the excess reagent. The bimolecular rate constants were obtained by monitoring the disappearance of Cl. The decay of the Cl signal as a function of the reaction distance was used to derive the observed first-order loss rate coefficient (*k*^l, s^{−1}).

Figure 3 shows a typical decay of Cl in the presence of isoprene. The experiment was performed at 8.7 Torr, with *Re* = 23. The initial concentration of Cl was estimated as 3.0 × 10⁹ molecule cm^{−3}, and the isoprene concentrations were varied between 4.0 × 10¹⁰ and 1.6 × 10¹¹ molecule cm^{−3}. From Figure 3, the observed first-order rate coefficients (*k*^l) were determined from the slopes of plots of the logarithm of Cl signal vs the injector distance and from the flow velocity. Such plots were linear for all of our experiments, indicating that secondary reactions occurred to a minimal extent. In our experiments there was a background signal at mass 35, which was subtracted from all of the points. We determined that the heterogeneous loss of chlorine atoms on the wall of the reactor was small, generally less than 1 s^{−1}. The effects of axial and radial diffusions of the reactants were estimated using the approach described by Brown.²⁷ Using the appropriate gas-phase diffusion coefficient for Cl, the correction due to gas-phase diffusion in the axial and radial directions was less than 3%. This correction was smaller than the random and systematic errors estimated in our experiments. Hence, for the data reported in this work we have obtained the bimolecular rate constant directly based on the observed first-order loss coefficient for Cl. The first-order rate coefficients were plotted against the isoprene concentration in Figure 4. The slope of the fit provides an effective bimolecular rate constant for the reaction between isoprene and Cl, corresponding to a value of 4.1 × 10^{−10} cm³ molecule^{−1} s^{−1}. Note that in Figure 3 the Cl concentration was reduced to about 30% of its original value at the highest isoprene concentration. Due to the existence of the background signal at *m/e* = 35 (about 10 to 15% of the original signal), we did not further increase the final Cl removal. This background signal was likely caused by the presence of HCl in our system.

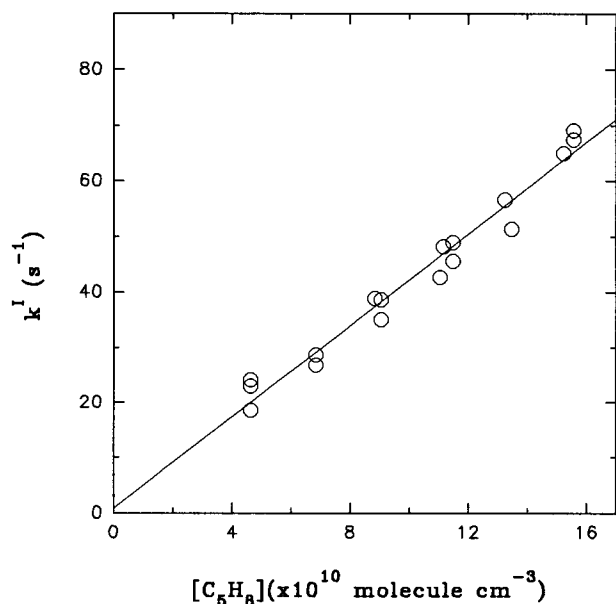


Figure 4. First-order loss rate coefficient k^1 as a function of isoprene concentration. Experimental conditions are similar to those in Figure 3.

Similar measurements were performed in the pressure range of 5 to 10 Torr, with values of (3.8 ± 0.4) , (4.0 ± 0.2) , (4.1 ± 0.2) , and $(4.1 \pm 0.3) \times 10^{-10} \text{ cm}^3 \text{ molecule}^{-1} \text{ s}^{-1}$ at 6.6, 8.2, 8.7, and 9.2 Torr, respectively. Each of the data represents at least four individual measurements at various initial concentrations of isoprene and Cl. Our averaged rate constant over the pressure range of 5 to 10 Torr is $(4.0 \pm 0.3) \times 10^{-10} \text{ cm}^3 \text{ molecule}^{-1} \text{ s}^{-1}$. The uncertainty represents the scatter in the data at the one standard deviation level and is not an estimate of the systematic errors. We estimate that systematic uncertainty in our measured rate constants is within $\pm 10\%$, considering the sources of error in the measurements (i.e., gas flows, temperature, detection signal, and pressure) and in the flow consideration.

Our measured rate constant between isoprene and Cl in the pressure range of 5 to 10 Torr is generally in good agreement with the results presently available in the literature.^{18–22} A summary of the previous measurements of the rate constants near room temperature is shown in Figure 5. Ragains and Finlayson-Pitts¹⁸ measured a rate constant of $(4.0 \pm 0.4) \times 10^{-10} \text{ cm}^3 \text{ molecule}^{-1} \text{ s}^{-1}$ at 5 Torr, in excellent agreement with the results reported in this study. Our value is slightly higher than those reported by Notario et al.²¹ and Bedjanian et al.,²² whose measured rates are $(3.6 \pm 0.4) \times 10^{-10} \text{ cm}^3 \text{ molecule}^{-1} \text{ s}^{-1}$ in the pressure range 15–60 Torr and $(3.4 \pm 0.5) \times 10^{-10} \text{ cm}^3 \text{ molecule}^{-1} \text{ s}^{-1}$ in the pressure range 0.25–3.0 Torr, respectively. The difference between our measured rate and those two latter studies, however, is within the quoted uncertainties of the respective work. Our results are also in good agreement with those recently measured by the NCAR kinetic group, whose measured values are $(4.0\text{--}5.0) \times 10^{-10} \text{ cm}^3 \text{ molecule}^{-1} \text{ s}^{-1}$ in the pressure range of 5 to 760 Torr.²⁸ In addition, another recently reported rate constant by Canosa-Mas et al. is $(4.0 \pm 0.8) \times 10^{-10} \text{ cm}^3 \text{ molecule}^{-1} \text{ s}^{-1}$ at 760 Torr.²⁰ Note that the largest disagreement for the reaction rate constant between Cl and isoprene among the various studies occurs at 760 Torr. For example, the value reported by Fantechi et al.¹⁹ is about 40% higher than that recently reported by Canosa-Mas et al.²⁰ Our measured rate constant in the pressure range of 5 to 10 Torr is very close to the value reported by Canosa-Mas et al.²⁰ at 760 Torr.

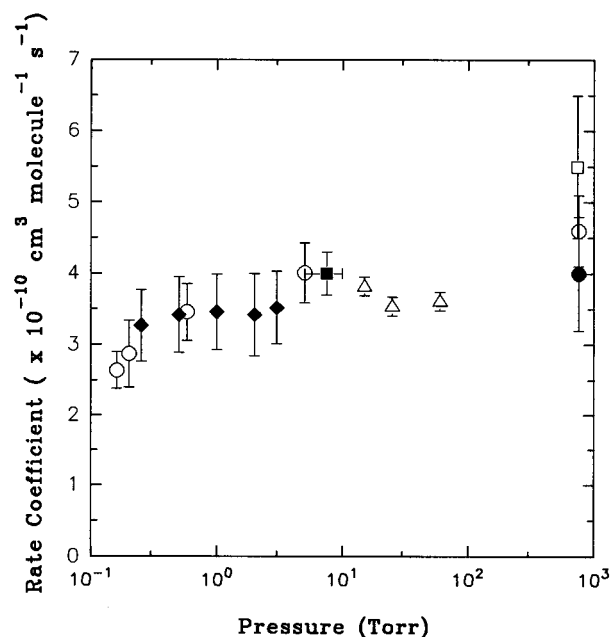


Figure 5. Bimolecular rate constant for the reaction of isoprene with Cl as a function of pressure. The different symbols are measurements reported by different investigators: solid square (this work), open circles (ref 18), open square (ref 19), solid circles (ref 20), open up-triangles (ref 21), and solid diamonds (ref 22).

Product Observation of Cl–Isoprene Reaction. Using the CIMS method we were able to directly monitor both products of reaction 1, HCl and the Cl–isoprene adduct. The product from reaction 1a was used to obtain the branching ratio based on the HCl formation. The measurement of the branching ratio was performed by monitoring the signal intensity of HCl, using an approach described by Bedjanian et al.²² Cl atoms were rapidly titrated by an excess of isoprene in the range of $(3 \text{ to } 11) \times 10^{11} \text{ molecule cm}^{-3}$. The increase in the HCl signal intensity ($[\Delta[\text{HCl}]]$) corresponded to the fraction of the consumed Cl concentration ($\Delta[\text{Cl}]$), as the isoprene concentration was varied. HCl was detected using the SF_6^- reagent ions as the $\text{HCl}\cdot\text{F}^-$ ions. HCl was calibrated using a 0.1% HCl/He mixture, with HCl collected from a concentrated HCl/ H_2SO_4 solution. The plot of the increase of the HCl signal as a function of $\Delta[\text{Cl}]$ yielded the branching ratio for reaction 1. The results for the branching ratio measurements were shown in Figure 6; the slope of the solid line yielded k_{1b}/k_1 , with a value of 0.177. Similar experiments were performed at other pressures in the range of 5 to 10 Torr, and the averaged branching ratio was $(17.4 \pm 4.0)\%$. The error represents uncertainty within 2σ and with an addition of 5% systematic error. At 298 K, the previously measured branching ratios are $(13.1 \pm 5.8)\%$ at 1 atm by Ragains and Finlayson-Pitts¹⁸ and $(16.9 \pm 2.2)\%$ in the pressure range of 0.3 to 3 Torr by Bedjanian et al.,²² respectively. The branching ratio we obtained in this study is hence in good agreement with those measured in previous studies.

Formation of the Cl–isoprene adduct was detected using the CIMS approach. In the previous study by Bedjanian et al.,²² it has been reported that the Cl–isoprene adduct is detected using electron impact (EI) as its parent ion. However, the ionization scheme using EI results in a significant fragmentation of this adduct due to the use of energetic electrons, which prohibits kinetic information to be derived. This problem, however, is avoided using the chemical ionization scheme. We have explored the ion–molecule reaction for the detection of the Cl–

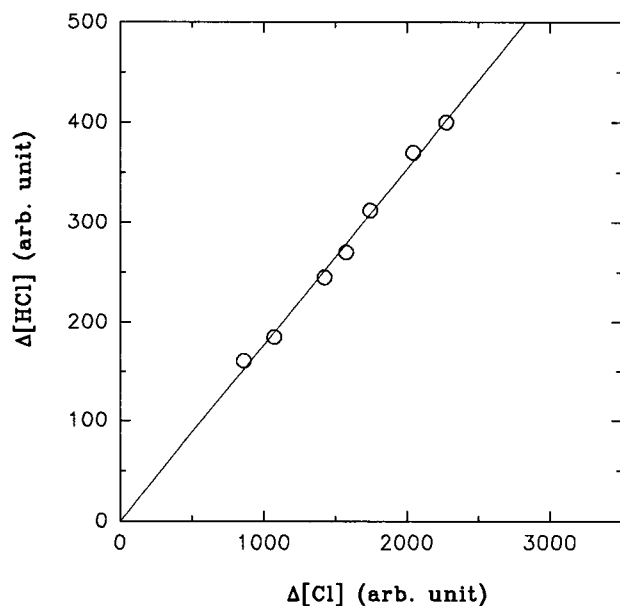


Figure 6. Increase of HCl versus consumed Cl concentration. Experimental conditions: $P = 10.1$ Torr, $U = 1164$ cm s $^{-1}$, and $Re = 14$.

isoprene adduct. This adduct can be detected with O_2^+ reagent ions according to the following ion–molecule reaction



Detection schemes similar to reaction 5 have been used to monitor the adduct radicals from the OH-initiated reactions of toluene and isoprene.^{26,29} The mass spectrometer is sensitive only to the mass of ions that are detected and does not discriminate between isomers. Indeed, addition of Cl to the double bonds of isoprene results in the formation of four possible isomeric radicals (Figure 1). Our ab initio calculations indicate that the most energetically favorable channel is via Cl addition to the C1- and C4-positions (by about 14 kcal mol $^{-1}$ less than that to the C2- and C3- positions),³⁰ consistent with experimental product studies for this reaction.^{18,19,22} Because the CIMS is incapable of discriminating the various isomers that were formed in our experiments, we referred the Cl-isoprene “adduct” to the species with mass 103 and atomic composition C_5H_8Cl . As to be discussed below, we believe that the isomeric effects on the overall rate constants would be negligible in our study.

Several procedures were taken to positively verify that the ions detected at $m/e = 103$ were indeed attributable to the Cl-isoprene adduct, rather than from secondary ion–molecule reactions. First, we observed that the signal at mass 103 disappeared when either the isoprene flow was stopped or when the microwave discharge for producing Cl atoms ceased. Those steps were necessary to ensure that this mass peak was related to the presence of isoprene or Cl radicals in the flow reactor. Alternatively, we monitored the 103 mass peak when the reaction time was successively increased. Figure 7 shows an example of the Cl-isoprene adduct formation, conducted at the following experimental conditions: $P = 9.2$ Torr, $Re = 15$, $U = 1341$ cm s $^{-1}$, and $[C_5H_8] = 7.5 \times 10^{11}$ molecule cm $^{-3}$. As is shown in this figure, there is a gradual increase in the Cl-isoprene adduct signal when the reaction distance is increased. Information such as that shown in Figure 7b can be employed to derive a rate coefficient for the reaction of Cl with isoprene. The procedure involves numerical simulation of the reaction system relevant to the present experiments using a computer

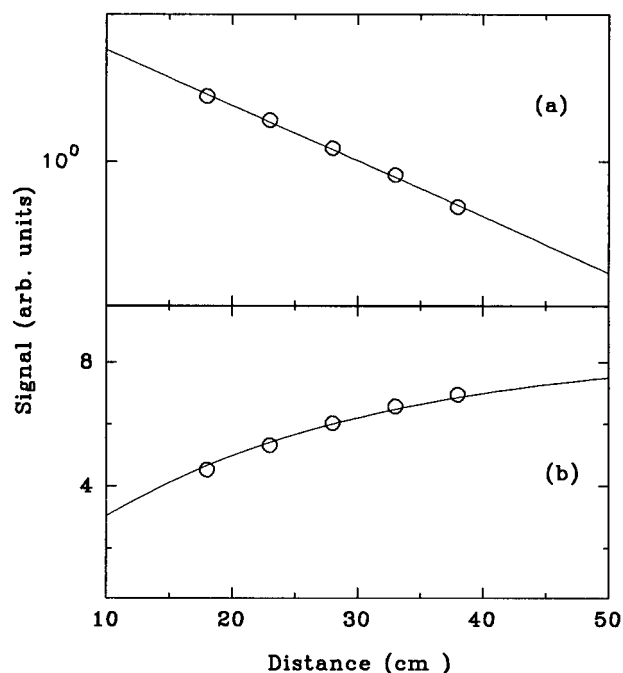


Figure 7. Variation of Cl (a) and Cl-isoprene adduct (b) signals as a function of reaction distance. The solid curves are from model calculations (see text). Experimental conditions are: $P = 9.6$ Torr, $U = 1424$ cm s $^{-1}$, $Re = 15$, and $[C_5H_8]_0 = 2.8 \times 10^{11}$ molecule cm $^{-3}$.

program.²⁶ The model input included the initial concentrations of Cl, isoprene, and all other precursors. The rate constant for reaction 1b was varied to fit the observed Cl-isoprene adduct formation profile, while we have used our measured branching ratio based on the HCl formation to constrain the fitting. Figures 7a and 7b show that the Cl-isoprene adduct signal at mass 103 rises in accordance with Cl disappearance. The Cl decay data as shown in Figure 7a correspond to an effective bimolecular rate of 4.1×10^{-10} cm 3 molecule $^{-1}$ s $^{-1}$. Note that for the results shown in Figure 7, the Cl decay and the adduct growth data were collected in separate runs, since either negative or positive reagent ions were used for the detection of Cl or the adduct. The solid line in Figure 7b represents the best fit to the observed production of the Cl-isoprene adduct; an effective bimolecular rate constant of 3.4×10^{-10} cm 3 molecule $^{-1}$ s $^{-1}$ was used in fitting the observed adduct formation profile. Using our measured branching ratio of 17.4%, the overall reaction rate between Cl and isoprene is 4.1×10^{-10} cm 3 molecule $^{-1}$ s $^{-1}$, consistent with the rate we measured based on the Cl decay. We estimated an uncertainty of 10% associated with fitting the Cl-isoprene adduction formation. On the basis of the product studies, we also concluded that the secondary reactions of the Cl-isoprene adduct were not important in our reaction system and that heterogeneous loss of this adduct on the surfaces of the flow reactor appeared to be minimal in our experiments. Recently, a similar approach has been recently used to investigate the adduct formation from the reactions between OH and isoprene and between OH and toluene.^{26,29}

Cl-Isoprene Adduct Reaction with O_2 . We have conducted measurements to examine the temporal evolution of the Cl-isoprene adduct in the presence of oxygen molecules, in an attempt to derive a rate constant between the Cl-isoprene adduct and O_2 . The experimental and modeling procedures were as follows. First, the production of the Cl-isoprene adduct was measured without O_2 , as the reaction time was successively increased, by monitoring the adduct signal at mass 103. The experiment was then repeated under the same conditions, except

TABLE 1: Summary of the Chemical Reactions Used in Computer Simulations for the System Involving Cl, Isoprene, and O₂

reaction	k ^a
C ₅ H ₈ + Cl → C ₅ H ₇ + HCl	6.6 × 10 ⁻¹¹ b
→ C ₅ H ₈ Cl	3.4 × 10 ⁻¹⁰ b
C ₅ H ₈ Cl + O ₂ → C ₅ H ₈ ClO ₂	1.0 × 10 ⁻¹⁴ b
Cl + O ₂ → ClO ₂	7.7 × 10 ⁻¹⁶
Cl + OCIO → ClO + ClO	5.8 × 10 ⁻¹¹
Cl + ClO ₂ → Cl ₂ + O ₂	2.3 × 10 ⁻¹⁰
→ ClO + ClO	1.2 × 10 ⁻¹¹
ClO + ClO → Cl ₂ O ₂	6.1 × 10 ⁻¹⁵
ClO + ClO → Cl ₂ + O ₂	4.8 × 10 ⁻¹⁵
→ ClOO + Cl	8.0 × 10 ⁻¹⁵
→ OCIO + Cl	3.5 × 10 ⁻¹⁵
ClO + OCIO → Cl ₂ O ₃	1.8 × 10 ⁻¹⁴

^a Rate constants are from ref 27 at 298 K and 9 Torr, except noted otherwise. ^b From this work.

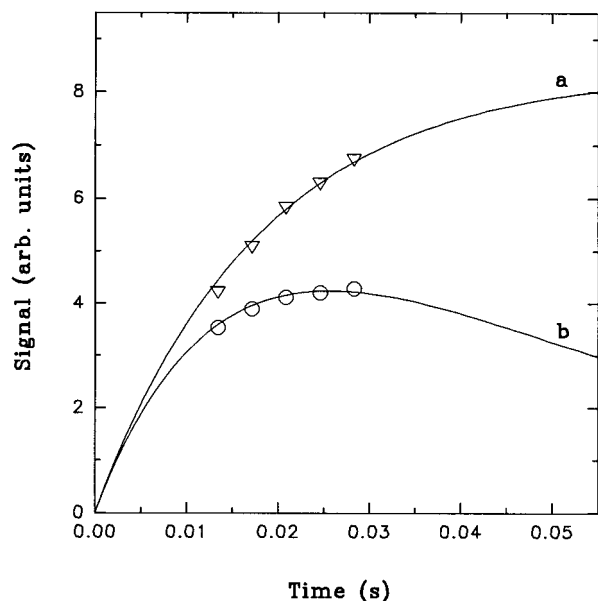


Figure 8. Production of the Cl-isoprene adduct as a function of the reaction time in the absence (triangles) and presence (circles) of O₂. The solid curves are from model calculations (see text). The initial concentrations of isoprene was 1.4 × 10¹¹ molecule cm⁻³. In (b) the concentration of O₂ molecules was 2.7 × 10¹⁵ molecule cm⁻³. The experiments were performed at P = 9.2 Torr, U = 1341 cm s⁻¹, and Re = 15.

with the addition of a known concentration O₂ in the flow reactor. By fitting the production of the Cl-isoprene adduct in the absence of O₂, a bimolecular rate constant for the formation of the Cl-isoprene adduct was determined. This rate constant (as well as our measured branching ratio) was then used to model the isoprene reaction system with the inclusion of the reaction of the Cl-isoprene adduct with O₂. A rate constant for the reaction between the Cl-isoprene adduct and O₂ was derived by best fitting the observed adduct production data in the presence of O₂. Table 1 lists the reactions and rate constants used in our simulations. The relevant kinetic rate constants were taken from the JPL publication.³¹

Figure 8 depicts the temporal evolution of the Cl-isoprene adduct with (open circles) and without O₂ (open triangles). The initial isoprene and O₂ concentrations were 1.4 × 10¹¹ and 2.7 × 10¹⁵ molecule cm⁻³, respectively. It is apparent in Figure 8 that the production of the Cl-isoprene adduct is reduced in the presence of O₂. This occurs because of the direct reaction between the Cl-isoprene adduct and O₂ to remove this adduct radical and to form the β-chloroalkenyl peroxy radicals. It is

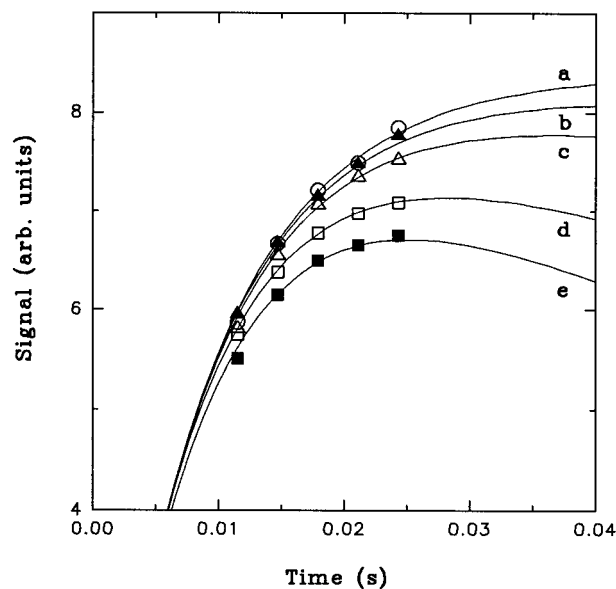


Figure 9. Production of the Cl-isoprene adduct as a function of reaction time at various O₂ concentrations (× 10¹⁵ molecule cm⁻³): (a) 0 (open circles), (b) 0.9 (solid up triangles), (c) 2.1 (open up triangles), (d) 5.8 (open squares), and (e) 8.9 (solid squares). The solid curves are from model calculations (see text). The initial concentration of isoprene was 2.7 × 10¹¹ molecule cm⁻³. The experiments were performed at P = 8.2 Torr, U = 1563 cm s⁻¹, and Re = 14.

believed that Cl addition to the terminal position of unsaturated double bond forms compounds with allylic resonance, and for these adducts facile addition of O₂ may take place at either of the two carbons.^{18,19} This process could result in the formation of six peroxy radicals (Figure 1). In Figure 8, the bimolecular reaction rate for the formation of the Cl-isoprene adduct by fitting the open triangles (solid curve) was used as 3.4 × 10⁻¹⁰ cm³ molecule⁻¹ s⁻¹, corresponding to an overall rate of 4.1 × 10⁻¹⁰ cm³ molecule⁻¹ s⁻¹. Using this value and fitting the Cl-isoprene adduct data in the presence of O₂ (open circles) allowed an estimation for the rate constant between the Cl-isoprene adduct with O₂, yielding a value of 1.0 × 10⁻¹⁴ cm³ molecule⁻¹ s⁻¹.

Figure 9 shows the production of the Cl-isoprene adduct as a function of O₂ concentrations from (0 to 8.9) × 10¹⁵ molecule cm⁻³ (curves a to e). The initial isoprene concentration was 2.7 × 10¹¹ molecule cm⁻³. Figure 9 illustrates that a larger deviation from curve a occurs at a higher O₂ concentration, reflecting a less production of the Cl-isoprene adduct at such a condition. At smaller O₂ concentrations less than about 8 × 10¹³ molecule cm⁻³, the observed adduct production was essentially nondistinguishable from that in the absence of O₂ molecules, indicating a negligible effect of O₂ on the adduct formation. The bimolecular rate constant of the reaction of the Cl-isoprene adduct with O₂ used in fitting all the data was 1.0 × 10⁻¹⁴ cm³ molecule⁻¹ s⁻¹. Similar experiments were performed under different conditions (i.e., different pressures, initial concentrations of O₂ and isoprene, etc.) The values are (1.0 ± 0.2) × 10⁻¹⁴ cm³ molecule⁻¹ s⁻¹ at 7.0 Torr and (1.0 ± 0.3) × 10⁻¹⁴ cm³ molecule⁻¹ s⁻¹ at 8.2, 9.3, and 10.2 Torr, respectively. Each of the data represents at least four individual measurements at various initial concentrations of isoprene, Cl, and O₂. The averaged rate constant for the reaction of the Cl-isoprene adduct with O₂ is hence (1.0 ± 0.3) × 10⁻¹⁴ cm³ molecule⁻¹ s⁻¹ over the pressure range of 5 to 10 Torr. The error is indicative of the scatter in the data at the one standard deviation level. We estimated a systematic error of about ± 50% for this reaction

in the present data. The source of errors included uncertainty associated with detection and modeling of the Cl–isoprene adduct, in addition to experimental uncertainties such as in the measurements of gas flows, temperature, and pressure and in the flow considerations.

In another recent study, we have used a similar approach to investigate the reaction between the OH–isoprene adduct and O₂ to form the β-hydroxyalkyl peroxy radicals,²⁶ with a rate constant of $2.8 \times 10^{-15} \text{ cm}^3 \text{ molecule}^{-1} \text{ s}^{-1}$. The rate constant for the reaction of the Cl–isoprene adduct with O₂ obtained in this study is hence higher than that of the reaction of OH–isoprene adduct with O₂. There are also some experimental kinetic results for the OH-initiated reactions of monoalkenes, dienes or trienes with nonconjugated >C=C< bonds; the resulting β-hydroxyalkyl radicals generally react rapidly with O₂, with the measured room-temperature rate constant in the range of $(3 \text{ to } 30) \times 10^{-12} \text{ cm}^3 \text{ molecule}^{-1} \text{ s}^{-1}$.^{1,32–34} On the other hand, for aromatic compounds (such as benzene and toluene), the reactions of hydroxycyclohexadienyl and alkyl-substituted hydroxycyclohexadienyl with O₂ have been shown to occur at very slow rates, on the order of $10^{-16} \text{ cm}^3 \text{ molecule}^{-1} \text{ s}^{-1}$.¹

Conclusions

We have presented kinetic results of the isoprene reactions initiated by Cl. The rate constants for the reaction of isoprene with Cl have been measured in the pressure range of 5 to 10 Torr and at $298 \pm 2 \text{ K}$. Direct product observations of HCl and the Cl–isoprene adduct have been made using the CIMS method. The Cl–isoprene adduct has been used to obtain the rate constant for the reaction between Cl and isoprene. By monitoring the production of the Cl–isoprene adduct in the presence of oxygen molecules, we have obtained the first experimental rate constant between O₂ and the Cl–isoprene adduct. Using our measured rate constant for the reaction between the Cl–isoprene adduct and O₂ and the atmospheric concentration of O₂ molecules at STP, the lifetime of the this adduct is estimated to be about $2 \times 10^{-5} \text{ s}$. Since this reaction may be pressure dependent, this lifetime corresponds to the upper limit. This implies that the reaction of the Cl–isoprene adduct with O₂ will be the dominant reaction pathway for this radical. Hence the photochemical oxidation of isoprene initiated by chlorine radicals provides an important mechanism for the formation of organic peroxy radicals in regions with large abundance of reactive chlorine. Subsequent reactions of the β-chloroalkenylperoxy radicals with nitric oxide (NO) can lead to tropospheric ozone formation.

Acknowledgment. This work was supported by a Grant from the Robert A. Welch Foundation (A-1417). The authors are grateful to J. J. Orlando and G. S. Tyndall of the NCAR kinetic

group for helpful discussions and for providing unpublished data on the Cl–isoprene reaction system. The referees have provided valuable comments for improving this manuscript.

References and Notes

- (1) Atkinson, R. *J. Phys. Chem. Ref. Data Monogr.* **1994**, 2, 1.
- (2) Seinfeld, J. H.; Pandis, S. N. *Atmospheric Chemistry and Physics: From Air Pollution to Climate Change*; John Wiley & Sons: New York, 1997.
- (3) Rasmussen, R. A.; Khalil, M. A. *J. Geophys. Res.* **1988**, 93, 1477.
- (4) Trainer, M.; Williams, E. J.; Parrish, D. D.; Buhr, M. P.; Allwine, E. J.; Westberg, H. H.; Fehsenfeld, F. C.; Liu, S. C. *Nature* **1987**, 329, 705.
- (5) Placet, M.; Battye, R. E.; Fehsenfeld, F. C.; Bassett, G. W. In *NAPAP SOST Rep. 1, Natl. Acid Precipitation Assessment Program*, Washington D.C., 1990.
- (6) Chameides, W. L.; Lindsay, R. W.; Richardson, J.; Kiang, C. S. *Science* **1988**, 241, 1473.
- (7) Jacob, D. J.; Wofsy, S. C., *J. Geophys. Res.* **1988**, 93, 1417.
- (8) Platt, U. In *European Commission 1997, The Oxidizing Capacity of the Troposphere*; Larson, B., Versino, B., Angeletti, G., Eds., 1997.
- (9) See, for example, Atkinson, R. *Atmos. Environ.* **2000**, 34, 2063, and references therein.
- (10) Graedel, T. E.; Keene, W. C. *J. Geophys. Res.* **1999**, 104, 8331.
- (11) Jobson, B. T.; Niki, H.; Yokouchi, Y.; Bottenheim, J.; Hopper, F.; Leitch, R. *J. Geophys. Res.* **1994**, 99, 25355.
- (12) Solberg, S.; Schmidbauer, N.; Semb, A.; Stordal, F.; Hov, O. *J. Atmos. Chem.* **1996**, 23, 301.
- (13) Wingenter, O. W.; Kubo, M. K.; Blake, N. J.; Smith, T. W.; Rowland, F. S. *J. Geophys. Res.* **1996**, 101, 4331.
- (14) Pszeeny, A. A. P.; Keene, W. C.; Jacob, D. J.; Fan, S.; Maben, J. R.; Zetwo, M. P.; Springer-Young, M.; Galloway, J. N. *Geophys. Res. Lett.* **1993**, 20, 699.
- (15) Singh, H. B.; Thakur, A. N.; Chen, Y. E.; Kanakidou, M. *Geophys. Res. Lett.* **1996**, 23, 1529.
- (16) Rudolph, J.; Koppmann, R.; Plass-Dulmer, Ch., *Atmos. Environ.* **1996**, 30, 1887.
- (17) Rudolph, J.; Ramacher, R.; Plass-Dulmer, Ch.; Muller, K. P.; Koppmann, R. *Tellus* **1997**, B49, 592.
- (18) Ragains, M. L.; Finlayson-Pitts, B. J. *J. Phys. Chem. A* **1997**, 101, 1509.
- (19) Fantechi, G.; Jensen, N. R.; Saastad, O.; Hjorth, J.; Peeters, J. *J. Atmos. Chem.* **1998**, 31, 247.
- (20) Canosa-Mas, C. E.; Hutton-Squire, H. R.; King, M. D.; Stewart, D. J.; Thompson, K. C.; Wayne, R. P. *J. Atmos. Chem.* **1999**, 34, 163.
- (21) Notario, A.; Le Bras, G.; Mellouki, A. *Chem. Phys. Lett.* **1997**, 281, 421.
- (22) Bedjanian, Y.; Laverdet, G.; Le Bras, G. *J. Phys. Chem. A* **1998**, 102, 953.
- (23) Keyser, L. F. *J. Phys. Chem.* **1984**, 88, 4750.
- (24) Zhang, R.; Molina, L. T.; Molina, M. J. *Rev. Sci. Instrum.* **1998**, 69, 4002.
- (25) Zhang, R.; Lei, W.; Molina, L. T.; Molina, M. J. *Int. J. Mass Spectrom. Ion Proc.* **2000**, 194, 41.
- (26) Zhang, R.; Suh, I.; Clinkenbeard, A.; Lei, W.; North, S. *J. Geophys. Res.*, in press.
- (27) Brown, R. L. *J. Res. Natl. Bur. Stand. (U. S.)* **1978**, 83, 1.
- (28) Orlando, J. J.; Tyndall, G. S., private communication, 1999.
- (29) Molina, M. J.; Zhang, R.; Broekhuizen, K.; Lei, W.; Navarro, R.; Molina, L. T. *J. Am. Chem. Soc.* **1999**, 121, 1(43), 10225.
- (30) Lei, W.; Zhang, R. *J. Chem. Phys.* **2000**, 113, 153.
- (31) DeMore, W. B.; Sander, S. P.; Howard, C. J.; Ravishankara, A. R.; Golden, D. M.; Kolb, C. E.; Hampson, R. F.; Kurylo, M. J.; Molina, M. J. *Chemical Kinetics and Photochemical Data for Use in Stratospheric Modeling*: JPL Publication 97–4, NASA, 1997.
- (32) Miyoshi, A.; Matsui, H.; Washida, N. *Chem. Phys. Lett.* **1989**, 160, 291.
- (33) Miyoshi, A.; Matsui, H.; Washida, N. *J. Phys. Chem.* **1990**, 94, 3016.
- (34) Lenhardt, T. M.; McDade, C. E.; Bayes, K. D. *J. Chem. Phys.* **1980**, 72, 304.